

Cite this: *Chem. Sci.*, 2025, 16, 21000

All publication charges for this article have been paid for by the Royal Society of Chemistry

## Ultrasound-triggered prodrug activation via sonochemically induced cleavage of a 3,5-dihydroxybenzyl carbamate scaffold

Xuancheng Fu,<sup>a</sup> Bowen Xu,<sup>a</sup> Hirusha Liyanage,<sup>a</sup> Cijun Zhang,<sup>a</sup> Warren F. Kincaid,<sup>a</sup> Amber L. Ford,<sup>a</sup> Luke G. Westbrook,<sup>a</sup> Seth D. Brown,<sup>a</sup> Tatum DeMarco,<sup>a</sup> James L. Houglund,<sup>ab</sup> John M. Franck<sup>a</sup> and Xiaoran Hu<sup>ab\*</sup>

Spatiotemporal control of drug release in deep tissues is crucial for targeted treatment precision and minimized systemic side effects. Ultrasound is a non-invasive and clinically safe stimulus capable of deep-tissue penetration without requiring optical transparency. Here, we introduce an innovative strategy for controlling cargo release via ultrasound-triggered sonochemical cleavage of a 3,5-dihydroxybenzyl carbamate (DHBC) prodrug platform. We demonstrate that low-intensity therapeutic ultrasound (LITUS) effectively generates hydroxyl radicals in aqueous solutions, which hydroxylate DHBC to initiate spontaneous cleavage and cargo release. Using a prototype chemotherapy prodrug (ProDOX) as a proof-of-concept, we show that LITUS irradiation triggers doxorubicin release to kill cancer cells *in vitro*. Remarkably, this sonochemical activation was successfully achieved through 2 cm of chicken breast, highlighting the deep-penetrating capability of our approach. Extending this strategy, we developed ProR848, a sono-activable prodrug of the Toll-like receptors (TLR) agonist R848, enabling remotely triggered, on-demand immune cell activation. Collectively, our results establish a novel and versatile sonochemical cleavage platform for ultrasound-targeted prodrug activation, offering significant potential for applications including controlled therapeutic release and responsive biomaterials.

Received 30th July 2025  
Accepted 18th September 2025

DOI: 10.1039/d5sc05710h

rsc.li/chemical-science

## Introduction

Achieving spatiotemporal control over cleavage chemistries deep within biological tissues is critically important for biomedical applications, such as site-specific drug release and dynamically tunable biomaterials.<sup>1–3</sup> However, current methods for remotely controlling chemical bond cleavage in deep tissue remain limited. Photo-responsive chemistry has been widely used to control drug release *in vitro* and on skin surfaces, but the limitation of tissue penetration hampers its application in deep tissues.<sup>4,5</sup> Radiation-controlled drug release has received increasing attention due to its deep-penetrating ability,<sup>6–8</sup> but it requires specialized equipment, and managing radiotherapy-associated side effects remains a significant concern. Ultrasound (U/S), mechanical sound waves beyond human hearing (20 kHz to MHz range), is widely used in biomedical fields such as deep-tissue imaging and oncology treatment.<sup>9–12</sup> Ultrasound as a stimulus features a unique combination of advantages: it operates remotely and non-invasively, penetrates deep tissues without needing optical transparency, offers precise targeting,

and utilizes cost-effective setups that have been proven safe in clinical applications.

Conventional ultrasound-targeted drug delivery systems harness the physical effects of acoustic waves, such as sonoporation (*i.e.*, ultrasound-induced formation of transient pores in cell membranes, improving membrane permeability) and enhanced extravasation, to improve local pharmacokinetics and drug biodistribution.<sup>13</sup> However, the utilization of active drugs still poses a risk of off-target side effects. An emerging strategy<sup>14</sup> addresses this challenge by employing ultrasound-controlled cleavage chemistry (Fig. 1) to activate covalently modified, nontoxic prodrugs exclusively at the target site, enabling localized activation of therapeutic effects while minimizing systemic drug exposure. One such approach (Fig. 1a) utilizes the sonodynamic effect (*i.e.*, ultrasonic generation of reactive oxygen species from sonosensitizers<sup>15–21</sup>) to induce chemical transformations for drug release.<sup>22–26</sup> However, the requirement for sonosensitizers increases formulation complexity in sonodynamic-based prodrug delivery systems. On the other hand, another ultrasound-mediated bond cleavage strategy (Fig. 1b) leverages the ultrasound-induced shear force field in solution to mechano-chemically activate force-sensitive structures, resulting in bond cleavage and cargo release.<sup>27–33</sup> Despite recent advancements in the field,<sup>34–36</sup> conventional polymer-mechanochemistry approaches often involve harsh, high-

<sup>a</sup>Department of Chemistry, BioInspired Institute, Syracuse University, Syracuse, New York, 13244, USA. E-mail: xhu156@syr.edu

<sup>b</sup>Department of Biology, Syracuse University, Syracuse, New York, 13244, USA



intensity ultrasonication conditions and necessitate the incorporation of long polymers to prodrug structures (restricting drug loading to <1 wt%), presenting challenges for clinical applicability.

Ultrasound-induced generation of hydroxyl radicals ( $\cdot\text{OH}$ ) in aqueous environments is a well-established phenomenon in sonochemistry.<sup>37–43</sup> Clinical acoustic conditions are known to cause acoustic cavitation both *in vivo* and *in vitro*.<sup>44–47</sup> This cavitation bubble, essentially a vacuum, collapses near-adiabatically and results in extreme pressures over 1000 atm and temperatures above 5000 K, while only slightly affecting the temperature of the bulk liquid. The extreme cavitation environment in collapsing cavitation bubbles serves as sonochemical micro-reactors and is sufficient to cause the pyrolysis of vapor molecules trapped in the bubble, generating primary radicals.<sup>48–51</sup> For example, Riesz used the methods of spin trapping electron spin resonance (ESR) to directly observe the formation of  $\cdot\text{OH}$  and  $\cdot\text{H}$  in the cavitation bubbles.<sup>42,47,52,53</sup> These primary radicals can either recombine or diffuse from the gas phase into the vicinity of the bubble and induce a wide variety of secondary chemical reactions in the bulk solution.<sup>54–60</sup> However, applying these intrinsic chemical effects of ultrasound to drive predictable and constructive chemistry for

biomedical applications remains an underexplored yet potentially transformative research venue.<sup>61</sup>

The hydroxyl radical ( $\cdot\text{OH}$ ), with a Hammett  $\sigma$  value of  $-0.41$ ,<sup>62</sup> is known to undergo electrophilic substitution reactions, and its ability to hydroxylate aromatic compounds has been studied primarily using  $\cdot\text{OH}$  generated by Fenton's reagent<sup>63,64</sup> or water radiolysis.<sup>65–67</sup> Recently, Liu and coworkers elegantly harnessed  $\cdot\text{OH}$  produced from radiolysis to hydroxylate an electron-rich 3,5-dihydroxybenzyl carbamate, triggering cascade chemical transformations that lead to the release of covalently conjugated drugs.<sup>65</sup> Inspired by ultrasound's intrinsic ability to generate  $\cdot\text{OH}$  radicals and the reactivity of  $\cdot\text{OH}$  in mediating radical hydroxylation,<sup>50,65</sup> we have developed a sonochemically controlled cleavage platform based on a 3,5-dihydroxybenzyl carbamate (DHBC) prodrug scaffold (Fig. 1c). Using a commercially available, FDA-registered low-intensity therapeutic ultrasound (LITUS) device, sonochemically generated  $\cdot\text{OH}$  radicals react with the DHBC *via* radical hydroxylation, triggering a subsequent elimination cascade that releases the molecular cargo. As a proof-of-concept, we synthesized a model prodrug **ProDOX** incorporating a chemotherapy drug doxorubicin (DOX), which is selectively activated under LITUS to release DOX and kill cancer cells *in vitro*. To demonstrate the deep-penetration ability of our strategy, we successfully activated **ProDOX** through a 2 cm thick chicken breast. Further, we extended the platform to immunotherapy by developing **ProR848**, a sono-activable prodrug of the toll-like receptor (TLR) agonist R848, designed to mitigate the systemic toxicity associated with TLR-based treatments. Upon LITUS irradiation, **ProR848** released active R848, selectively activating tumor-associated macrophages (TAMs) and dendritic cells (DCs), as evidenced by upregulation of pro-inflammatory markers and inflammatory cytokine secretion. Together, these chemotherapeutic and immunotherapeutic applications demonstrate the versatility and effectiveness of our deep-penetrating, ultrasound-triggered cleavage platform, offering significant potential for applications ranging from controlled therapeutic release to responsive biomaterials.

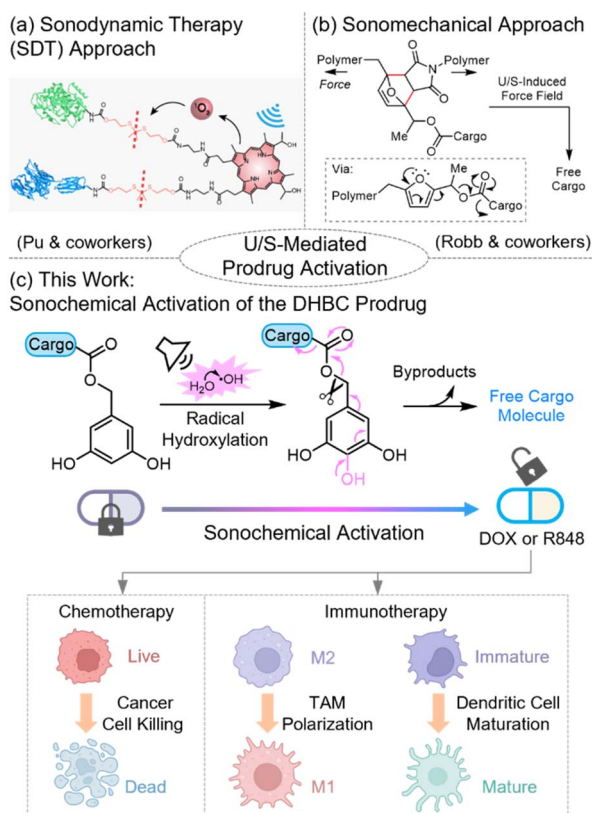


Fig. 1 An overview of ultrasound-mediated prodrug activation strategies. This work introduces a sonochemical approach that harnesses the intrinsic chemical effects of ultrasound in aqueous solutions to activate DHBC prodrugs *via* a radical hydroxylation mechanism. Fig. 1a is adapted with permission from ref. 24. Copyright 2022, Springer Nature.

## Results and discussion

We first investigated the sonochemical production of  $\cdot\text{OH}$  radicals using an FDA-registered, commercially available ultrasound device. Under our standard LITUS conditions (frequency: 1 MHz; power: 1.0 W cm<sup>2</sup>; duty cycle: 50%) (see SI for mechanical index calculations and biosafety discussions), the generation of  $\cdot\text{OH}$  in the acoustically irradiated PBS buffer solutions was monitored using ESR with 5,5-dimethyl-1-pyrroline-N-oxide (DMPO), a  $\cdot\text{OH}$ -specific spin trap that forms a well-understood DMPO-OH spin adduct in presence of  $\cdot\text{OH}$  radicals.<sup>53</sup> LITUS irradiation produced a new set of four-line peaks (Fig. 2a) which are characteristic of the hyperfine coupling in the DMPO-OH adduct, while DMPO-OOH signals were not seen. Comparison with reported hyperfine coupling constants<sup>68</sup> as well as simulated ESR spectrum (Fig. S1) confirms that these new peaks correspond to the expected DMPO-OH spin adduct. From ESR spin-counting analysis (see



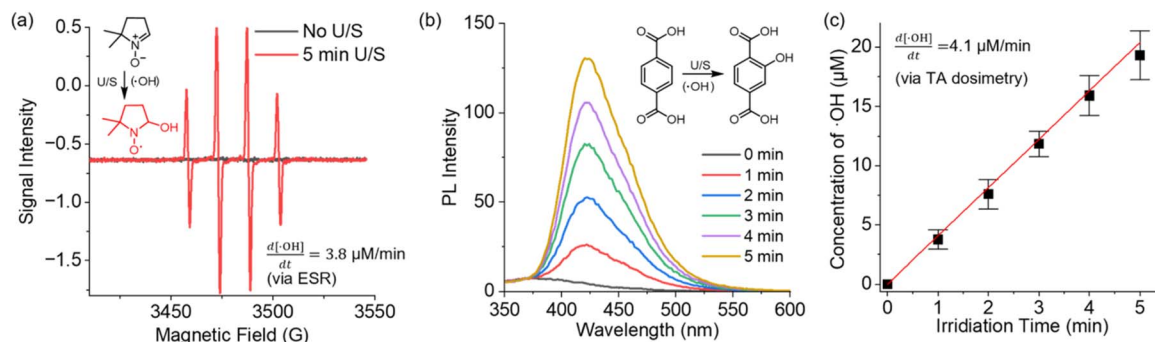


Fig. 2 (a) ESR spectra of a 5 mM solution of DMPO in PBS before and after sonication. (b) Sonochemical conversion of TA (20 mM in PBS) to hTA monitored by fluorescence spectroscopy. (c) Concentration of sonochemical  $\cdot\text{OH}$  as a function of sonication time, calculated by multiplying the concentration of hTA by 1/0.35.

SI for details), the concentration of DMPO-OH was determined to be  $18.8 \mu\text{M}$  after 5 min sonication of a 5 mM DMPO solution.

We further performed a quantitative study of ultrasonic  $\cdot\text{OH}$  generation using an established terephthalic acid (TA) dosimetry method—the nonfluorescent TA readily reacts with  $\cdot\text{OH}$  to yield fluorescent 2-hydroxyterephthalic acid (hTA).<sup>69,70</sup> The fluorescence emission of an irradiated TA solution linearly increased in the first five minutes of ultrasonication (Fig. 2b and c), indicating the steady sonochemical conversion of TA to hTA. It is understood that about 35% of sonochemical  $\cdot\text{OH}$  radicals react with TA to produce hTA,<sup>71,72</sup> and therefore, the concentration of  $\cdot\text{OH}$  produced in 5 minutes of ultrasonication was calculated to be  $20.4 \mu\text{M}$  ( $4.1 \mu\text{M min}^{-1}$ ), which aligns closely with that estimated by ESR. To confirm the radical nature of the observed hydroxylation of TA, we conducted a control experiment using a highly reactive radical quencher, hydroquinone

(rate constant of  $11 \times 10^9 \text{ M}^{-1} \text{ s}^{-1}$  with  $\cdot\text{OH}$ ).<sup>73</sup> The addition of 100 mM hydroquinone into a 20 mM TA solution near completely inhibited TA hydroxylation, confirming the key role of radicals (Fig. S5).

Following the sonochemical TA dosimetry experiments, we explored the potential of harnessing sonochemical  $\cdot\text{OH}$  to trigger the radical hydroxylation and cascade molecular release from a DHBC-based model prodrug **Pro1**. Electron-rich DHBC motifs are designed to react with sonochemically generated  $\cdot\text{OH}$  through a radicalphilic reaction, triggering a cascade elimination process that releases the 4-nitroaniline payload (Fig. 3a).<sup>65</sup> The release of 4-nitroaniline results in the emergence of a characteristic absorption around 400 nm, providing a convenient signal for monitoring its release using UV-vis spectroscopy. As shown in Fig. 3b, ultrasound irradiation of a  $50 \mu\text{M}$  solution of **Pro1** in PBS results in an absorbance increase

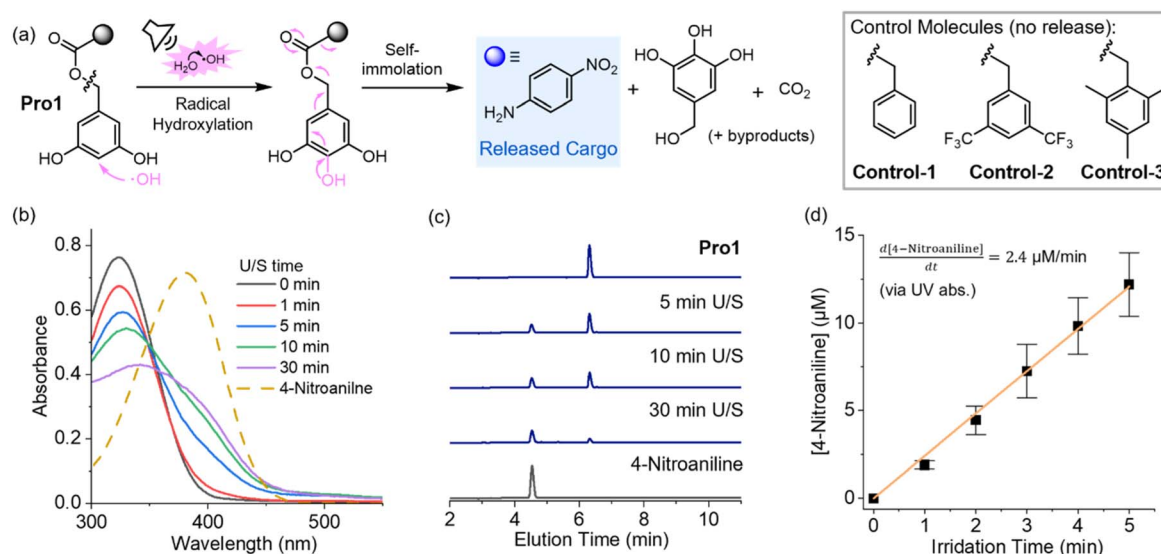


Fig. 3 (a) Ultrasonic activation of **Pro1** mediated by sonochemical  $\cdot\text{OH}$  radicals. For simplicity, only the hydroxylation reaction at the 4-position is depicted, although hydroxylation at the 2-position is also possible (Fig. S6).<sup>65</sup> Structures of control molecules are also shown. (b) Absorption spectra of a  $50 \mu\text{M}$  solution of **Pro1** in PBS as a function of sonication time. The dashed curve corresponds to the absorbance of a separately prepared  $50 \mu\text{M}$  solution of 4-nitroaniline. (c) Sonolysis of **Pro1** monitored by HPLC. (d) The concentration of free 4-nitroaniline in the **Pro1** solution in the first 5 minutes of ultrasound irradiation, calculated from the absorbance increase at 400 nm.



around 400 nm, corresponding to nitroaniline release. HPLC measurements further confirmed the identity of 4-nitroaniline (Fig. 3c). The rate of 4-nitroaniline release in the first 5 min was estimated at  $2.4 \mu\text{M min}^{-1}$  based on absorbance measurements (Fig. 3d), indicating this model DHBC prodrug was effectively activated under our sonochemical conditions to release the cargo molecules. The release of 4-nitroaniline plateaued at approximately  $22 \mu\text{M}$  after 20 min sonication (Fig. S8). The incomplete conversion is anticipated due to nonspecific sonochemical side reactions—sonochemical degradation of both **Pro1** and the released nitroaniline can occur in or near the cavitation microbubbles, which feature extreme environments. Currently, we are unable to identify the sonochemical byproduct(s).

We conducted a series of control experiments to validate the proposed sonolysis mechanism. By introducing 100 mM hydroquinone (radical quencher) into the **Pro1** solution, ultrasound-triggered cargo release from **Pro1** was inhibited (Fig. S10), supporting that the observed sonochemical activation of **Pro1** is through a radical mechanism. Additionally, we designed **Control-1/2/3** molecules where the electron-rich 3,5-dihydroxybenzyl motif was replaced: **Control-1** and **Control-2** contain a less 'OH-reactive benzyl motif and 3,5-bis(trifluoromethyl)benzyl motif, respectively, while **Control-3** comprises a 2,4,6-trimethylbenzyl group, whose hydroxylation product is inactive toward the elimination cascade (Fig. S12). Irradiation of **Control-1/2/3** molecules under identical acoustic conditions as used for **Pro1** lead to minor increase in 4-nitroaniline absorbance (Fig. S11). HPLC analysis also confirmed the

absence of cargo release from sonicated control molecules (Fig. S12).

As a proof of concept, we demonstrated ultrasound-triggered release of a cytotoxic chemotherapy drug DOX from the sonochemically responsive DHBC prodrug platform (Fig. 4a). This prototype model prodrug **ProDOX** was exposed to standard LITUS irradiation, with the reaction monitored by HPLC equipped with a UV detector (monitored at 254 nm). The sonicated solutions displayed a distinct peak at around 4.3 min elution time, corresponding to free DOX released from the activated prodrug (Fig. S14). The DOX peak steadily increased during the first five minutes of ultrasonication, reaching a peak concentration of around  $0.5 \mu\text{M}$ . However, prolonged sonication reduced the DOX concentration, presumably due to the nonspecific sonolysis of DOX under cavitation conditions (Fig. 4b). The appearance of the inflection point for DOX concentration matches the trend observed for 4-nitroaniline release from **Pro1** (Fig. S8). Given the electron-rich, anthraquinone structure of DOX, it is particularly susceptible to nonspecific degradation under sonochemical conditions (Fig. S15).

While future research will explore the structure-activity relationships affecting the sonochemical stability of therapeutically active structures and will identify candidates with enhanced resistance to sonolysis, the efficacy of our current prototype model prodrug is sufficient to demonstrate the ultrasound-controlled DOX release for *in vitro* cancer treatment. *HeLa* cells were treated *in vitro* by solutions of **ProDOX**, with or

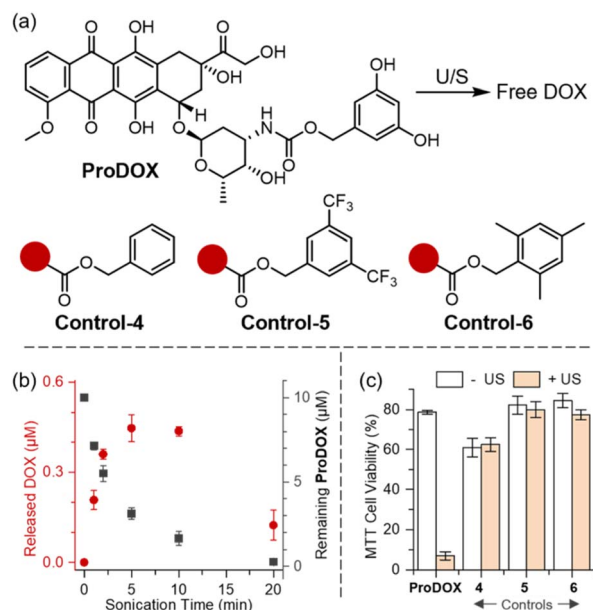


**Fig. 4** (a) Structures of **ProDOX** and control prodrugs. (b) Concentration of released DOX from a solution of  $10 \mu\text{M}$  **ProDOX** in PBS as a function of sonication time. (c) MTT viability assay results demonstrate increased cytotoxicity in LITUS-irradiated **ProDOX** solution, compared to a nonirradiated **ProDOX** solution. This ultrasound-induced cytotoxicity is not observed in control prodrugs.

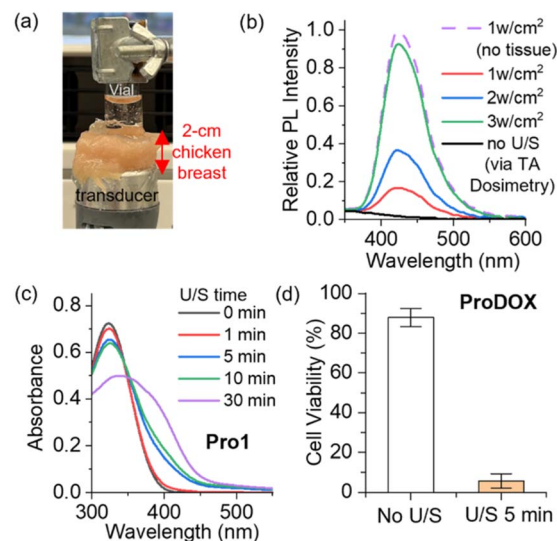


**Fig. 5** (a) A photograph showing our setup applying LITUS through a 2 cm thick chicken breast tissue to a solution. (b) Fluorescence spectra of 20 mM TA solutions after 5 min of LITUS irradiation at varied sound intensity (1 MHz, 50% duty cycle) applied through chicken breast. All traces are normalized relative to the fluorescence of a TA solution sonicated ( $1 \text{ W cm}^{-2}$ , 5 min) without chicken breast (dashed line). (c) Absorption spectra monitoring the release of 4-nitroaniline from a  $50 \mu\text{M}$  **Pro1** solution as a function of sonication ( $3 \text{ W cm}^{-2}$ , through chicken breast). (d) MTT viability assay with *HeLa* cells show LITUS-induced ( $3 \text{ W cm}^{-2}$ , through chicken breast) cytotoxicity of **ProDOX**.



without ultrasonic irradiation (Fig. 4c, left). Only the sonicated **ProDOX** (yellow bar) exhibited significant cytotoxicity, confirming that ultrasonic irradiation activated the cytotoxicity of **ProDOX**. Meanwhile, control groups with DOX masked by various benzyl derivatives showed limited toxicity both in the presence and in the absence of sonication, with HPLC confirming no DOX release (Fig. S14).

Then, we demonstrate the tissue-penetration ability of our controlled-release techniques by remotely manipulating the chemical transformation of prodrugs using LITUS through a 2 cm-thick chicken breast (Fig. 5a). Through the animal tissue, our standard  $1 \text{ W cm}^{-2}$  LITUS condition successfully triggered the hydroxylation of TA as indicated by fluorescence turn-on, while moderately increased acoustic intensity at  $3 \text{ W cm}^{-2}$  exhibits more pronounced sonochemical effects (Fig. 5b)—this  $3 \text{ W cm}^{-2}$  intensity was used in all tissue-penetrating experiments. Ultrasound irradiation applied through the chicken breast successfully triggered the release of 4-nitroaniline from **Pro1** (Fig. 5c) as well as DOX from **ProDOX** (Fig. S18). Ultrasound applied through chicken breast effectively activated **ProDOX** solutions, enhancing their cytotoxicity against *HeLa* cells *in vitro* (Fig. 5d).

TLR agonists represent potent immunotherapeutic agents capable of enhancing immune activation and remodeling immunosuppressive tumor microenvironments.<sup>74,75</sup> This effect is primarily mediated through the activation of immune cells, particularly by polarizing tumor-associated macrophages (TAMs) from an anti-inflammatory, pro-tumoral M2-like phenotype to a pro-inflammatory, anti-tumoral M1-like phenotype.<sup>76–78</sup> However, systemic administration of TLR agonists is limited clinically by severe side effects, notably cytokine storm.<sup>79</sup> Therefore, strategies enabling targeted release of TLR agonists have shown great potential to confine immune activation to the tumor site and reduce systemic toxicity.<sup>80–85</sup> Herein, we leverage our sono-responsive DHBC platform to precisely control the release of the TLR agonist (R848) under LITUS. Our pro-agonist, **ProR848**, demonstrates outstanding biocompatibility towards TAMs, exhibiting negligible toxicity at  $10 \mu\text{M}$  (Fig. S19a). Evaluation of inflammatory markers CD86 and CD80 revealed that TAMs activation by  $1 \mu\text{M}$  **ProR848** was minimal (Fig. S19b and c), indicating its potential for minimizing systemic immune activation. Subsequent LITUS-mediated activation of  $1 \mu\text{M}$  **ProR848** was monitored using HPLC (Fig. 6a). Ultrasonicated samples exhibited a distinct

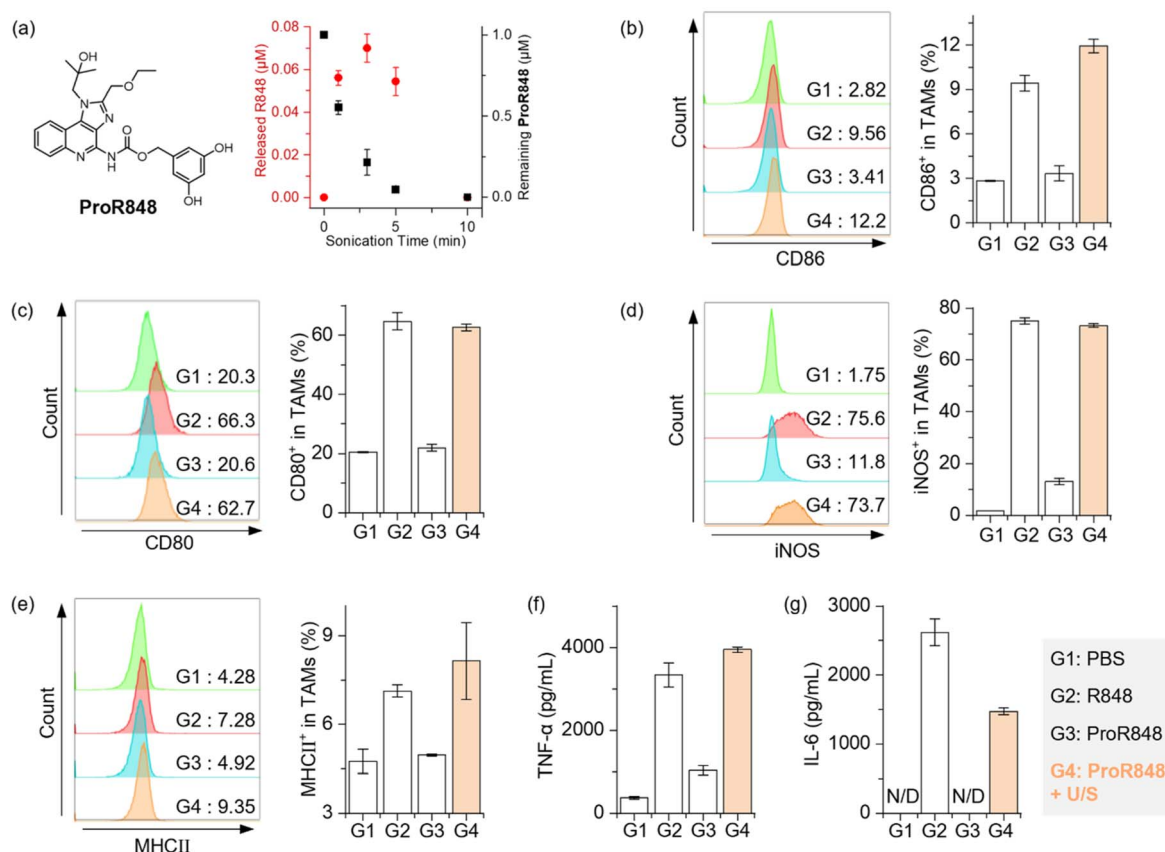


**Fig. 6** (a) Structures of **ProR848** and concentration of released R848 from a solution of  $1 \mu\text{M}$  **ProR848** in PBS as a function of sonication time (1 MHz, 50% duty cycle,  $1 \text{ W cm}^{-2}$ ), quantified by HPLC. (b–e) Flow cytometry analysis showing enhanced expression of pro-inflammatory markers on tumor-associated macrophages (TAMs) after treatment with **ProR848** activated by 3 min ultrasound irradiation (G4, orange bars), compared with PBS negative control (G1), free R848 positive control ( $0.07 \mu\text{M}$ , G2), and non-sonicated **ProR848** (G3): (b) CD86, (c) CD80, (d) iNOS, (e) MHC class II. (f and g) ELISA measurements demonstrating secretion of pro-inflammatory cytokines from TAM supernatants after various treatments (G1 to G4): (f) TNF- $\alpha$ , (g) IL-6.



chromatographic peak at approximately 6.6 min (Fig. S20), indicative of the release of active R848 cargos. R848 release peaked at approximately 0.07  $\mu\text{M}$  within the first three minutes of sonication and subsequently decreased upon prolonged irradiation (Fig. 6a).

Having confirmed LITUS-triggered R848 release, we evaluated its ability to induce TAMs polarization. PBS-treated and 0.07  $\mu\text{M}$  R848-treated groups served as negative and positive controls, respectively. Flow cytometric analysis demonstrated that ultrasound-activated **ProR848** (G4, orange bars) significantly upregulated pro-inflammatory markers CD86, CD80, and inducible nitric oxide synthase (iNOS) in TAMs, mirroring the response elicited by free R848 (G2) treatment (Fig. 6b–d). In contrast, TAMs exposed to non-sonicated **ProR848** (G3) exhibited marker expression comparable to PBS controls (G1), demonstrating that the TAMs polarization was due to LITUS-mediated drug release. Additionally, a substantial enhancement in major histocompatibility complex class II (MHCII) expression endowed macrophages with augmented antigen-presenting capabilities, facilitating improved activation and maturation of CD4<sup>+</sup> helper T cells and subsequent adaptive immune responses (Fig. 6e).<sup>86,87</sup> The immunostimulatory efficacy of **ProR848** under LITUS irradiation was further corroborated by enzyme-linked immunosorbent assay (ELISA) data, revealing significantly elevated secretion of proinflammatory cytokines tumor necrosis factor-alpha (TNF- $\alpha$ ) and interleukin-6 (IL-6) following ultrasound treatment (Fig. 6f and g).

Dendritic cells (DCs) are another immune cell type with important roles in orchestrating innate and adaptive immunity. We further evaluated the effects of ultrasound-activated **ProR848** on DC maturation using the DC2.4 cell line. Similar to TAMs, DC2.4 cells exhibited excellent tolerance to 1  $\mu\text{M}$  **ProR848**, without evidence of DCs maturation (Fig. S21a and b). Remarkably, upon ultrasound exposure, significant maturation of DC2.4 cells was observed, as evidenced by pronounced increases in MHCII expression (Fig. S21c). Collectively, our results demonstrate that LITUS-triggered R848 release from **ProR848** effectively activates TAMs and promotes DCs maturation. This strategy enables on-demand and localized immune cell activation and holds promise for targeted immunotherapy with reduced systemic immune-related adverse effects.

## Conclusions

This work introduces a sonochemical strategy to control prodrug activation through ultrasound-triggered cleavage of a DHBC prodrug platform. Using a commercially available, FDA-registered therapeutic ultrasound device, we demonstrated that our standard LITUS conditions generate  $\cdot\text{OH}$  radicals at a rate of several  $\mu\text{M min}^{-1}$ . The DHBC prodrug scaffold is designed to undergo radical hydroxylation by these sonochemically generated  $\cdot\text{OH}$  radicals, triggering a self-immolative cascade to release the cargo molecule. Using a chemotherapy prodrug model **ProDOX** as a proof-of-concept, we show that LITUS irradiation triggers DOX release, effectively killing *HeLa* cells *in vitro*. Notably, sonochemical manipulation of the DHBC prodrugs was successfully achieved through a layer of chicken

breast, highlighting the deep-penetration capability of our approach. Moreover, to address systemic toxicity associated with TLR agonists in immunotherapy, we developed a LITUS-activable prodrug **ProR848**. Upon LITUS activation, **ProR848** released R848 and induced the polarization of TAMs and maturation of DC cells, demonstrating the potential to trigger localized immunostimulatory activity through our sonochemical strategy. Together, these results demonstrate the versatility of our sonochemical cleavage platform for controlled release of chemotherapy and immunomodulatory drugs, offering potential for targeted delivery in deep tissues inaccessible by conventional noninvasive stimuli. Future work will focus on understanding structure-sonochemical reactivity relationships in bioactive substances and designing prodrug molecules with enhanced resistance to unspecific sonolysis.

## Ethical statements

All experimental procedures, including chemical synthesis, analytical measurements, cell culture studies, and experiments with chicken breast tissue were conducted in compliance with the relevant national regulations and institutional guidelines at Syracuse University (approval committees include the Environmental Health and Safety Services, the Institutional Biosafety Committee, and the Institutional Animal Care and Use Committee).

## Author contributions

X. Fu led the study and contributed to the manuscript writing. B. Xu, H. Liyanage, C. Zhang, W. F. Kincaid, A. L. Ford, L. G. Westbrook, S. D. Brown, and T. DeMarco contributed to the experimental work. J. L. Houglund and J. M. Franck supervised students and provided research resources. X. Hu conceived and oversaw the project, secured funding and resources, and contributed to the manuscript writing.

## Conflicts of interest

There are no conflicts to declare.

## Data availability

Supplementary information: experimental details, supporting figures, synthetic procedures, UV-vis, fluorescence, HPLC, and NMR spectra. See DOI: <https://doi.org/10.1039/d5sc05710h>.

## Acknowledgements

Financial support from Syracuse University (SU) is gratefully acknowledged. JLH acknowledges financial support from NIH grant GM134102. Undergraduate student L. G. Westbrook was funded by the Syracuse University Office of Undergraduate Research & Creative Engagement (SOURCE). The authors acknowledge that elements of Fig. 1 and the TOC graphic were created with <https://www.BioRender.com> (Created in



BioRender). Fu, X. (2025) <https://www.BioRender.com/typ1wme>.

## References

- 1 J. Kost and R. Langer, Responsive Polymer Systems for Controlled Delivery of Therapeutics, *Trends Biotechnol.*, 1992, **10**, 127–131, DOI: [10.1016/0167-7799\(92\)90194-Z](https://doi.org/10.1016/0167-7799(92)90194-Z).
- 2 S. Mura, J. Nicolas and P. Couvreur, Stimuli-Responsive Nanocarriers for Drug Delivery, *Nature Mater.*, 2013, **12**(11), 991–1003, DOI: [10.1038/nmat3776](https://doi.org/10.1038/nmat3776).
- 3 J. Wang, X. Wang, X. Fan and P. R. Chen, Unleashing the Power of Bond Cleavage Chemistry in Living Systems, *ACS Cent. Sci.*, 2021, **7**(6), 929–943, DOI: [10.1021/acscentsci.1c00124](https://doi.org/10.1021/acscentsci.1c00124).
- 4 T. Dvir, M. R. Banghart, B. P. Timko, R. Langer and D. S. Kohane, Photo-Targeted Nanoparticles, *Nano Lett.*, 2010, **10**(1), 250–254, DOI: [10.1021/nl903411s](https://doi.org/10.1021/nl903411s).
- 5 W. A. Velema, W. Szymanski and B. L. Feringa, Photopharmacology: Beyond Proof of Principle, *J. Am. Chem. Soc.*, 2014, **136**(6), 2178–2191, DOI: [10.1021/ja413063e](https://doi.org/10.1021/ja413063e).
- 6 Q. Fu, S. Zhang, S. Shen, Z. Gu, J. Chen, D. Song, P. Sun, C. Wang, Z. Guo, Y. Xiao, Y. Q. Gao, Z. Guo and Z. Liu, Radiotherapy-Triggered Reduction of Platinum-Based Chemotherapeutic Prodrugs in Tumours, *Nat. Biomed. Eng.*, 2024, **8**(11), 1425–1435, DOI: [10.1038/s41551-024-01239-x](https://doi.org/10.1038/s41551-024-01239-x).
- 7 Q. Fu, Z. Gu, S. Shen, Y. Bai, X. Wang, M. Xu, P. Sun, J. Chen, D. Li and Z. Liu, Radiotherapy Activates Picolinium Prodrugs in Tumours, *Nat. Chem.*, 2024, **16**(8), 1348–1356, DOI: [10.1038/s41557-024-01501-4](https://doi.org/10.1038/s41557-024-01501-4).
- 8 X.-Y. Cui, Z. Li, Z. Kong, Y. Liu, H. Meng, Z. Wen, C. Wang, J. Chen, M. Xu, Y. Li, J. Gao, W. Zhu, Z. Hao, L. Huo, S. Liu, Z. Yang and Z. Liu, Covalent Targeted Radioligands Potentiate Radionuclide Therapy, *Nature*, 2024, **630**(8015), 206–213, DOI: [10.1038/s41586-024-07461-6](https://doi.org/10.1038/s41586-024-07461-6).
- 9 A. Lakshmanan, Z. Jin, S. P. Nety, D. P. Sawyer, A. Lee-Gosselin, D. Malounda, M. B. Swift, D. Maresca and M. G. Shapiro, Acoustic Biosensors for Ultrasound Imaging of Enzyme Activity, *Nat. Chem. Biol.*, 2020, **16**(9), 988–996, DOI: [10.1038/s41589-020-0591-0](https://doi.org/10.1038/s41589-020-0591-0).
- 10 Y. Wu, Y. Liu, Z. Huang, X. Wang, Z. Jin, J. Li, P. Limsakul, L. Zhu, M. Allen, Y. Pan, R. Bussell, A. Jacobson, T. Liu, S. Chien and Y. Wang, Control of the Activity of CAR-T Cells within Tumours via Focused Ultrasound, *Nat. Biomed. Eng.*, 2021, **5**(11), 1336–1347, DOI: [10.1038/s41551-021-00779-w](https://doi.org/10.1038/s41551-021-00779-w).
- 11 A. Bar-Zion, A. Nourmahnad, D. R. Mittelstein, S. Shivaiei, S. Yoo, M. T. Buss, R. C. Hurt, D. Malounda, M. H. Abedi, A. Lee-Gosselin, M. B. Swift, D. Maresca and M. G. Shapiro, Acoustically Triggered Mechanotherapy Using Genetically Encoded Gas Vesicles, *Nat. Nanotechnol.*, 2021, **16**(12), 1403–1412, DOI: [10.1038/s41565-021-00971-8](https://doi.org/10.1038/s41565-021-00971-8).
- 12 D. P. Sawyer, A. Bar-Zion, A. Farhadi, S. Shivaiei, B. Ling, A. Lee-Gosselin and M. G. Shapiro, Ultrasensitive Ultrasound Imaging of Gene Expression with Signal Unmixing, *Nat. Methods*, 2021, **18**(8), 945–952, DOI: [10.1038/s41592-021-01229-w](https://doi.org/10.1038/s41592-021-01229-w).
- 13 J. Castle, M. Butts, A. Healey, K. Kent, M. Marino and S. B. Feinstein, Ultrasound-Mediated Targeted Drug Delivery: Recent Success and Remaining Challenges, *Am. J. Physiol.: Heart Circ. Physiol.*, 2013, **304**(3), H350–H357, DOI: [10.1152/ajpheart.00265.2012](https://doi.org/10.1152/ajpheart.00265.2012).
- 14 X. Fu and X. Hu, Ultrasound-Controlled Prodrug Activation: Emerging Strategies in Polymer Mechanochemistry and Sonodynamic Therapy, *ACS Appl. Bio Mater.*, 2024, **4**(00150), DOI: [10.1021/acsabm.4c00150](https://doi.org/10.1021/acsabm.4c00150).
- 15 W. Wang, X. Wu, K. W. Kevin Tang, I. Pyatnitskiy, R. Taniguchi, P. Lin, R. Zhou, S. L. C. Capocyan, G. Hong and H. Wang, Ultrasound-Triggered *In Situ* Photon Emission for Noninvasive Optogenetics, *J. Am. Chem. Soc.*, 2023, **145**(2), 1097–1107, DOI: [10.1021/jacs.2c10666](https://doi.org/10.1021/jacs.2c10666).
- 16 Y. Lyu, Q. Li, S. Xie, Z. Zhao, L. Ma, Z. Wu, W. Bao, Y. Cai, H. Liu, H. He, K. Xie, F. Gao, Y. Yang, P. Wu, P. He, K. Wang, X. Dai, H. Wu, T. Lan and C. Cheng, Synergistic Ultrasound-Activable Artificial Enzyme and Precision Gene Therapy to Suppress Redox Homeostasis and Malignant Phenotypes for Controllably Combating Hepatocellular Carcinoma, *J. Am. Chem. Soc.*, 2025, **147**(3), 2350–2368, DOI: [10.1021/jacs.4c10997](https://doi.org/10.1021/jacs.4c10997).
- 17 F. Chen, S. Ren, L. Huang, Q. Wu, M. Li, S. Li, J. Gao, Y. Lai, Z. Cai, X. Liu, W. Tao, T. Lammers, Z. Xu and H. Yu, Ultrasound-Activatable Lipid Nanoplatform for Region-Confinned Innate Immune Stimulation and mRNA Vaccination Therapy of Cancer, *J. Am. Chem. Soc.*, 2025, DOI: [10.1021/jacs.5c06028](https://doi.org/10.1021/jacs.5c06028).
- 18 Z. Wu, L. Zhang, Z. Wang, S. Liu, Q. Zhang, C. Shi, Y. Wang, G. Xu, D. Zhu, M. R. Bryce, L. Ren and B. Z. Tang, Sonodynamic and Bioorthogonal Sonocatalytic Thrombotic Therapy Based on AIE Cationic Tetranuclear Ir(III) Complex Nanoplatform Guided by NIR-Chemiluminescence Imaging, *Adv. Mater.*, 2025, **37**, 2503599, DOI: [10.1002/adma.202503599](https://doi.org/10.1002/adma.202503599).
- 19 S. Liu, J. Li, A. Wang, D. K. P. Ng and N. Zheng, Multicomponent Polymerization toward Poly(BODIPY-Sulfonamide)s as Unique SO<sub>2</sub> Generators for Sonodynamic and Gas Combination Therapy, *Angew. Chem., Int. Ed.*, 2025, **64**(13), e202422362, DOI: [10.1002/anie.202422362](https://doi.org/10.1002/anie.202422362).
- 20 Z. Yang, Z. Jiao, Z. Chen, C. Qiao, C. Huang, L. Wang, Z. Rao, R. Zhang and Z. Wang, Programmable Bacterial Architects Crafting Sonosensitizers for Tumor-Specific Sonodynamic Immunotherapy, *Adv. Mater.*, 2025, **37**(32), 2504206, DOI: [10.1002/adma.202504206](https://doi.org/10.1002/adma.202504206).
- 21 M. He, Z. Ma, L. Zhang, Z. Zhao, Z. Zhang, W. Liu, R. Wang, J. Fan, X. Peng and W. Sun, Sonoinduced Tumor Therapy and Metastasis Inhibition by a Ruthenium Complex with Dual Action: Superoxide Anion Sensitization and Ligand Fracture, *J. Am. Chem. Soc.*, 2024, **146**(37), 25764–25779, DOI: [10.1021/jacs.4c08278](https://doi.org/10.1021/jacs.4c08278).
- 22 J. Yu, S. He, C. Zhang, C. Xu, J. Huang, M. Xu and K. Pu, Polymeric STING Pro-Agonists for Tumor-Specific Sonodynamic Immunotherapy, *Angew. Chem., Int. Ed.*, 2023, **62**(32), e202307272, DOI: [10.1002/anie.202307272](https://doi.org/10.1002/anie.202307272).



- 23 J. Wu and K. Pu, Leveraging Semiconducting Polymer Nanoparticles for Combination Cancer Immunotherapy, *Adv. Mater.*, 2024, **36**(1), 2308924, DOI: [10.1002/adma.202308924](https://doi.org/10.1002/adma.202308924).
- 24 C. Zhang, J. Huang, Z. Zeng, S. He, P. Cheng, J. Li and K. Pu, Catalytical Nano-Immuno-complexes for Remote-Controlled Sono-Metabolic Checkpoint Trimodal Cancer Therapy, *Nat. Commun.*, 2022, **13**(1), 3468, DOI: [10.1038/s41467-022-31044-6](https://doi.org/10.1038/s41467-022-31044-6).
- 25 L. Liu, J. Zhang, R. An, Q. Xue, X. Cheng, Y. Hu, Z. Huang, L. Wu, W. Zeng, Y. Miao, J. Li, Y. Zhou, H.-Y. Chen, H. Liu and D. Ye, Smart Nanosensitizers for Activatable Sono-Photodynamic Immunotherapy of Tumors by Redox-Controlled Disassembly, *Angew. Chem., Int. Ed.*, 2023, **62**(10), e202217055, DOI: [10.1002/anie.202217055](https://doi.org/10.1002/anie.202217055).
- 26 H. Xu, M. Zheng, D. Ye, J. An, Z. Liu, Z. Tang and X. Chen, Ultrasound-Triggered Activation of p-Azidobenzyloxycarbonyl-Based Prodrugs via Radical-Mediated Cascade Elimination, *J. Am. Chem. Soc.*, 2025, **147**(24), 20667–20679, DOI: [10.1021/jacs.5c03878](https://doi.org/10.1021/jacs.5c03878).
- 27 X. Hu, T. Zeng, C. C. Husic and M. J. Robb, Mechanically Triggered Small Molecule Release from a Masked Furfuryl Carbonate, *J. Am. Chem. Soc.*, 2019, **141**(38), 15018–15023, DOI: [10.1021/jacs.9b08663](https://doi.org/10.1021/jacs.9b08663).
- 28 X. Hu, T. Zeng, C. C. Husic and M. J. Robb, Mechanically Triggered Release of Functionally Diverse Molecular Payloads from Masked 2-Furylcarbinol Derivatives, *ACS Cent. Sci.*, 2021, **7**(7), 1216–1224, DOI: [10.1021/acscentsci.1c00460](https://doi.org/10.1021/acscentsci.1c00460).
- 29 S. Huo, P. Zhao, Z. Shi, M. Zou, X. Yang, E. Warszawik, M. Loznik, R. Göstl and A. Herrmann, Mechanochemical Bond Scission for the Activation of Drugs, *Nat. Chem.*, 2021, **13**(2), 131–139, DOI: [10.1038/s41557-020-00624-8](https://doi.org/10.1038/s41557-020-00624-8).
- 30 G. Kim, Q. Wu, J. L. Chu, E. J. Smith, M. L. Oelze, J. S. Moore and K. C. Li, Ultrasound Controlled Mechanophore Activation in Hydrogels for Cancer Therapy, *Proc. Natl. Acad. Sci. U. S. A.*, 2022, **119**(4), e2109791119, DOI: [10.1073/pnas.2109791119](https://doi.org/10.1073/pnas.2109791119).
- 31 Y. Sun, W. J. Neary, Z. P. Burke, H. Qian, L. Zhu and J. S. Moore, Mechanically Triggered Carbon Monoxide Release with Turn-On Aggregation-Induced Emission, *J. Am. Chem. Soc.*, 2022, **144**(3), 1125–1129, DOI: [10.1021/jacs.1c12108](https://doi.org/10.1021/jacs.1c12108).
- 32 L. Chen, R. Nixon and G. De Bo, Force-Controlled Release of Small Molecules with a Rotaxane Actuator, *Nature*, 2024, **628**(8007), 320–325, DOI: [10.1038/s41586-024-07154-0](https://doi.org/10.1038/s41586-024-07154-0).
- 33 B. A. Versaw, T. Zeng, X. Hu and M. J. Robb, Harnessing the Power of Force: Development of Mechanophores for Molecular Release, *J. Am. Chem. Soc.*, 2021, **143**(51), 21461–21473, DOI: [10.1021/jacs.1c11868](https://doi.org/10.1021/jacs.1c11868).
- 34 Y. Yao, M. E. McFadden, S. M. Luo, R. W. Barber, E. Kang, A. Bar-Zion, C. A. B. Smith, Z. Jin, M. Legendre, B. Ling, D. Malounda, A. Torres, T. Hamza, C. E. R. Edwards, M. G. Shapiro and M. J. Robb, Remote Control of Mechanochemical Reactions under Physiological Conditions Using Biocompatible Focused Ultrasound, *Proc. Natl. Acad. Sci. U. S. A.*, 2023, **120**(39), e2309822120, DOI: [10.1073/pnas.2309822120](https://doi.org/10.1073/pnas.2309822120).
- 35 A. Ishaqat, J. Hahmann, C. Lin, X. Zhang, C. He, W. H. Rath, P. Habib, S. E. M. Sahnoun, K. Rahimi, R. Vinokur, F. M. Mottaghy, R. Göstl, M. Bartneck and A. Herrmann, In Vivo Polymer Mechanochemistry with Polynucleotides, *Adv. Mater.*, 2024, **36**(32), 2403752, DOI: [10.1002/adma.202403752](https://doi.org/10.1002/adma.202403752).
- 36 J. Fan, R. Lennarz, K. Zhang, A. Mourran, J. Meisner, M. Xuan, R. Göstl and A. Herrmann, Polymer Microbubbles as Universal Platform to Accelerate Polymer Mechanochemistry, *Nat. Commun.*, 2025, **16**(1), 5380, DOI: [10.1038/s41467-025-60667-8](https://doi.org/10.1038/s41467-025-60667-8).
- 37 K. S. Suslick and G. J. Price, APPLICATIONS OF ULTRASOUND TO MATERIALS CHEMISTRY, *Annu. Rev. Mater. Sci.*, 1999, **29**(1), 295–326, DOI: [10.1146/annurev.matsci.29.1.295](https://doi.org/10.1146/annurev.matsci.29.1.295).
- 38 A. Henglein, Sonochemistry: Historical Developments and Modern Aspects, *Ultrasonics*, 1987, **25**(1), 6–16, DOI: [10.1016/0041-624X\(87\)90003-5](https://doi.org/10.1016/0041-624X(87)90003-5).
- 39 V. Mišić and P. Riesz, Free Radical Intermediates in Sonodynamic Therapy, *Ann. N. Y. Acad. Sci.*, 2000, **899**(1), 335–348, DOI: [10.1111/j.1749-6632.2000.tb06198.x](https://doi.org/10.1111/j.1749-6632.2000.tb06198.x).
- 40 C. L. Christman, A. J. Carmichael, M. M. Mossoba and P. Riesz, Evidence for Free Radicals Produced in Aqueous Solutions by Diagnostic Ultrasound, *Ultrasonics*, 1987, **25**(1), 31–34, DOI: [10.1016/0041-624X\(87\)90008-4](https://doi.org/10.1016/0041-624X(87)90008-4).
- 41 L. J. M. Juffermans, P. A. Dijkmans, R. J. P. Musters, C. A. Visser and O. Kamp, Transient Permeabilization of Cell Membranes by Ultrasound-Exposed Microbubbles Is Related to Formation of Hydrogen Peroxide, *Am. J. Physiol.: Heart Circ. Physiol.*, 2006, **291**(4), H1595–H1601, DOI: [10.1152/ajpheart.01120.2005](https://doi.org/10.1152/ajpheart.01120.2005).
- 42 P. Riesz, D. Berdahl and C. L. Christman, Free Radical Generation by Ultrasound in Aqueous and Nonaqueous Solutions, *Environ. Health Perspect.*, 1985, **64**, 233–252, DOI: [10.1289/ehp.8564233](https://doi.org/10.1289/ehp.8564233).
- 43 R. F. Martínez, G. Cravotto and P. Cintas, Organic Sonochemistry: A Chemist's Timely Perspective on Mechanisms and Reactivity, *J. Org. Chem.*, 2021, **86**(20), 13833–13856, DOI: [10.1021/acs.joc.1c00805](https://doi.org/10.1021/acs.joc.1c00805).
- 44 A. Sazgarnia, A. Shanei, H. Eshghi, M. Hassanzadeh-Khayyat, H. Esmaily and M. M. Shanei, Detection of Sonoluminescence Signals in a Gel Phantom in the Presence of Protoporphyrin IX Conjugated to Gold Nanoparticles, *Ultrasonics*, 2013, **53**(1), 29–35, DOI: [10.1016/j.ultras.2012.03.009](https://doi.org/10.1016/j.ultras.2012.03.009).
- 45 Y. He, D. Xing, S. Tan, Y. Tang and K. Ueda, In Vivo Sonoluminescence Imaging with the Assistance of FCLA, *Phys. Med. Biol.*, 2002, **47**(9), 1535–1541, DOI: [10.1088/0031-9155/47/9/308](https://doi.org/10.1088/0031-9155/47/9/308).
- 46 Y. He, D. Xing, G. Yan and K. Ueda, FCLA Chemiluminescence from Sonodynamic Action *in Vitro* and *in Vivo*, *Cancer Lett.*, 2002, **182**(2), 141–145, DOI: [10.1016/S0304-3835\(02\)00070-8](https://doi.org/10.1016/S0304-3835(02)00070-8).
- 47 K. Makino, M. M. Mossoba and P. Riesz, Formation of •OH and •H in Aqueous Solutions by Ultrasound Using Clinical



- Equipment, *Radiat. Res.*, 1983, **96**(2), 416, DOI: [10.2307/3576225](https://doi.org/10.2307/3576225).
- 48 K. S. Suslick, Sonochemistry, *Science*, 1990, **247**(4949), 1439–1445, DOI: [10.1126/science.247.4949.1439](https://doi.org/10.1126/science.247.4949.1439).
- 49 K. S. Suslick, S. J. Doktycz and E. B. Flint, On the Origin of Sonoluminescence and Sonochemistry, *Ultrasonics*, 1990, **28**(5), 280–290, DOI: [10.1016/0041-624X\(90\)90033-K](https://doi.org/10.1016/0041-624X(90)90033-K).
- 50 *Sonochemistry and Sonoluminescence*, ed. Crum, L. A., Mason, T. J., Reisse, J. L. and Suslick, K. S., Springer Netherlands, Dordrecht, 1999. DOI: [10.1007/978-94-015-9215-4](https://doi.org/10.1007/978-94-015-9215-4).
- 51 N. Miyoshi, T. Igarashi and P. Riesz, Evidence against Singlet Oxygen Formation by Sonolysis of Aqueous Oxygen-Saturated Solutions of Hematoporphyrin and Rose Bengal, *Ultrason. Sonochem.*, 2000, **7**(3), 121–124, DOI: [10.1016/S1350-4177\(99\)00042-5](https://doi.org/10.1016/S1350-4177(99)00042-5).
- 52 V. Mišák, N. Miyoshi and P. Riesz, EPR Spin Trapping Study of the Decomposition of Azo Compounds in Aqueous Solutions by Ultrasound: Potential for Use as Sonodynamic Sensitizers for Cell Killing, *Free Radical Res.*, 1996, **25**(1), 13–22, DOI: [10.3109/10715769609145652](https://doi.org/10.3109/10715769609145652).
- 53 V. Mišák and P. Riesz, Recent Applications of EPR and Spin Trapping to Sonochemical Studies of Organic Liquids and Aqueous Solutions, *Ultrason. Sonochem.*, 1996, **3**(3), S173–S186, DOI: [10.1016/S1350-4177\(96\)00023-5](https://doi.org/10.1016/S1350-4177(96)00023-5).
- 54 E. L. Mead, R. G. Sutherland and R. E. Verrall, Ultrasonic Degradation of Thymine, *J. Chem. Soc., Chem. Commun.*, 1973, **13**, 414, DOI: [10.1039/c39730000414](https://doi.org/10.1039/c39730000414).
- 55 K. Okitsu, M. Ashokkumar and F. Grieser, Sonochemical Synthesis of Gold Nanoparticles: Effects of Ultrasound Frequency, *J. Phys. Chem. B*, 2005, **109**(44), 20673–20675, DOI: [10.1021/jp0549374](https://doi.org/10.1021/jp0549374).
- 56 M. Bradley, M. Ashokkumar and F. Grieser, Sonochemical Production of Fluorescent and Phosphorescent Latex Particles, *J. Am. Chem. Soc.*, 2003, **125**(2), 525–529, DOI: [10.1021/ja0268581](https://doi.org/10.1021/ja0268581).
- 57 K. Vinodgopal, M. Ashokkumar and F. Grieser, Sonochemical Degradation of a Polydisperse Nonylphenol Ethoxylate in Aqueous Solution, *J. Phys. Chem. B*, 2001, **105**(16), 3338–3342, DOI: [10.1021/jp004178j](https://doi.org/10.1021/jp004178j).
- 58 J. Berlan, F. Trabelsi, H. Delmas, A. M. Wilhelm and J. F. Petrigiani, Oxidative Degradation of Phenol in Aqueous Media Using Ultrasound, *Ultrason. Sonochem.*, 1994, **1**(2), S97–S102, DOI: [10.1016/1350-4177\(94\)90005-1](https://doi.org/10.1016/1350-4177(94)90005-1).
- 59 A. Weissler, Ultrasonic Hydroxylation in a Fluorescence Analysis for Microgram Quantities of Benzoic Acid, *Nature*, 1962, **193**(4820), 1070, DOI: [10.1038/1931070a0](https://doi.org/10.1038/1931070a0).
- 60 M. Ashokkumar, D. Sunartio, S. Kentish, R. Mawson, L. Simons, K. Vilku and C. Versteeg, (Kees). Modification of Food Ingredients by Ultrasound to Improve Functionality: A Preliminary Study on a Model System, *Innovative Food Sci. Emerging Technol.*, 2008, **9**(2), 155–160, DOI: [10.1016/j.ifset.2007.05.005](https://doi.org/10.1016/j.ifset.2007.05.005).
- 61 Y. Tong, M. Li, H. Huang, S. Long, W. Sun, J. Du, J. Fan, L. Wang, B. Liu and X. Peng, Urea-Bond Scission Induced by Therapeutic Ultrasound for Biofunctional Molecule Release, *J. Am. Chem. Soc.*, 2022, **144**(37), 16799–16807, DOI: [10.1021/jacs.2c03669](https://doi.org/10.1021/jacs.2c03669).
- 62 M. Anbar, D. Meyerstein and P. Neta, The Reactivity of Aromatic Compounds toward Hydroxyl Radicals, *J. Phys. Chem.*, 1966, **70**(8), 2660–2662, DOI: [10.1021/j100880a034](https://doi.org/10.1021/j100880a034).
- 63 H. Kaur and B. Halliwell [6] Detection of Hydroxyl Radicals by Aromatic Hydroxylation. In *Methods in Enzymology*, Elsevier, 1994; Vol. 233, pp. 67–82. DOI: [10.1016/S0076-6879\(94\)33009-3](https://doi.org/10.1016/S0076-6879(94)33009-3).
- 64 T. Kurata, Y. Watanabe, M. Katoh and Y. Sawaki, Mechanism of Aromatic Hydroxylation in the Fenton and Related Reactions. One-Electron Oxidation and the NIH Shift, *J. Am. Chem. Soc.*, 1988, **110**(22), 7472–7478, DOI: [10.1021/ja00230a032](https://doi.org/10.1021/ja00230a032).
- 65 Q. Fu, H. Li, D. Duan, C. Wang, S. Shen, H. Ma and Z. Liu, External-Radiation-Induced Local Hydroxylation Enables Remote Release of Functional Molecules in Tumors, *Angew. Chem., Int. Ed.*, 2020, **59**(48), 21546–21552, DOI: [10.1002/anie.202005612](https://doi.org/10.1002/anie.202005612).
- 66 G. Albarran, E. Mendoza and R. H. Schuler, Concerted Effects of Substituents in the Reaction of •OH Radicals with Aromatics: The Hydroxybenzaldehydes, *Radiat. Phys. Chem.*, 2016, **124**, 46–51, DOI: [10.1016/j.radphyschem.2015.11.022](https://doi.org/10.1016/j.radphyschem.2015.11.022).
- 67 X.-M. Pan, M. N. Schuchmann and C. Von Sonntag, Oxidation of Benzene by the OH Radical. A Product and Pulse Radiolysis Study in Oxygenated Aqueous Solution, *J. Chem. Soc., Perkin Trans. 1*, 1993, **2**(3), 289, DOI: [10.1039/p29930000289](https://doi.org/10.1039/p29930000289).
- 68 S. K. Jackson, M. P. Thomas, S. Smith, M. Madhani, S. C. Rogers and P. E. James, In Vivo EPR Spectroscopy: Biomedical and Potential Diagnostic Applications, *Faraday Discuss.*, 2004, **126**(0), 103–117, DOI: [10.1039/B307162F](https://doi.org/10.1039/B307162F).
- 69 T. J. Mason, J. P. Lorimer, D. M. Bates and Y. Zhao, Dosimetry in Sonochemistry: The Use of Aqueous Terephthalate Ion as a Fluorescence Monitor, *Ultrason. Sonochem.*, 1994, **1**(2), S91–S95, DOI: [10.1016/1350-4177\(94\)90004-3](https://doi.org/10.1016/1350-4177(94)90004-3).
- 70 D. B. Rajamma, S. Anandan, N. S. M. Yusof, B. G. Pollet and M. Ashokkumar, Sonochemical Dosimetry: A Comparative Study of Weissler, Fricke and Terephthalic Acid Methods, *Ultrason. Sonochem.*, 2021, **72**, 105413, DOI: [10.1016/j.ultsonch.2020.105413](https://doi.org/10.1016/j.ultsonch.2020.105413).
- 71 X. Fang, G. Mark and C. von Sonntag, OH Radical Formation by Ultrasound in Aqueous Solutions Part I: The Chemistry Underlying the Terephthalate Dosimeter, *Ultrason. Sonochem.*, 1996, **3**(1), 57–63, DOI: [10.1016/1350-4177\(95\)00032-1](https://doi.org/10.1016/1350-4177(95)00032-1).
- 72 F. Tampieri, M.-P. Ginebra and C. Canal, Quantification of Plasma-Produced Hydroxyl Radicals in Solution and Their Dependence on the pH, *Anal. Chem.*, 2021, **93**(8), 3666–3670, DOI: [10.1021/acs.analchem.0c04906](https://doi.org/10.1021/acs.analchem.0c04906).
- 73 J. D. Smith, H. Kinney and C. Anastasio, Aqueous Benzene-Diols React with an Organic Triplet Excited State and Hydroxyl Radical to Form Secondary Organic Aerosol, *Phys. Chem. Chem. Phys.*, 2015, **17**(15), 10227–10237, DOI: [10.1039/C4CP06095D](https://doi.org/10.1039/C4CP06095D).
- 74 Applications and clinical trial landscape using Toll-like receptor agonists to reduce the toll of cancer | *npj Precis.*



- Oncol.* <https://www.nature.com/articles/s41698-023-00364-1>, accessed 2025-06-30.
- 75 S. Bhagchandani, J. A. Johnson and D. J. Irvine, Evolution of Toll-like Receptor 7/8 Agonist Therapeutics and Their Delivery Approaches: From Antiviral Formulations to Vaccine Adjuvants, *Adv. Drug Delivery Rev.*, 2021, **175**, 113803, DOI: [10.1016/j.addr.2021.05.013](https://doi.org/10.1016/j.addr.2021.05.013).
- 76 W. Zhang, M. Wang, C. Ji, X. Liu, B. Gu and T. Dong, Macrophage Polarization in the Tumor Microenvironment: Emerging Roles and Therapeutic Potentials, *Biomed. Pharmacother.*, 2024, **177**, 116930, DOI: [10.1016/j.biopha.2024.116930](https://doi.org/10.1016/j.biopha.2024.116930).
- 77 C. B. Rodell, S. P. Arlauckas, M. F. Cuccarese, C. S. Garris, R. Li, M. S. Ahmed, R. H. Kohler, M. J. Pittet and R. Weissleder, TLR7/8-Agonist-Loaded Nanoparticles Promote the Polarization of Tumour-Associated Macrophages to Enhance Cancer Immunotherapy, *Nat. Biomed. Eng.*, 2018, **2**(8), 578–588, DOI: [10.1038/s41551-018-0236-8](https://doi.org/10.1038/s41551-018-0236-8).
- 78 X. Fu, Y. Huang, H. Zhao, E. Zhang, Q. Shen, Y. Di, F. Lv, L. Liu and S. Wang, Near-Infrared-Light Remote-Controlled Activation of Cancer Immunotherapy Using Photothermal Conjugated Polymer Nanoparticles, *Adv. Mater.*, 2021, **33**(34), 2102570, DOI: [10.1002/adma.202102570](https://doi.org/10.1002/adma.202102570).
- 79 J. Nie, L. Zhou, W. Tian, X. Liu, L. Yang, X. Yang, Y. Zhang, S. Wei, D. W. Wang and J. Wei, Deep Insight into Cytokine Storm: From Pathogenesis to Treatment, *Signal Transduction Targeted Ther.*, 2025, **10**(1), 112, DOI: [10.1038/s41392-025-02178-y](https://doi.org/10.1038/s41392-025-02178-y).
- 80 J. Li, X. Yu, Y. Jiang, S. He, Y. Zhang, Y. Luo and K. Pu, Second Near-Infrared Photothermal Semiconducting Polymer Nanoadjuvant for Enhanced Cancer Immunotherapy, *Adv. Mater.*, 2021, **33**(4), 2003458, DOI: [10.1002/adma.202003458](https://doi.org/10.1002/adma.202003458).
- 81 Y. Jiang, J. Huang, C. Xu and K. Pu, Activatable Polymer Nanoagonist for Second Near-Infrared Photothermal Immunotherapy of Cancer, *Nat. Commun.*, 2021, **12**(1), 742, DOI: [10.1038/s41467-021-21047-0](https://doi.org/10.1038/s41467-021-21047-0).
- 82 J. Wan, L. Ren, X. Li, S. He, Y. Fu, P. Xu, F. Meng, S. Xian, K. Pu and H. Wang, Photoactivatable Nanoagonists Chemically Programmed for Pharmacokinetic Tuning and *in Situ* Cancer Vaccination, *Proc. Natl. Acad. Sci. U. S. A.*, 2023, **120**(8), e2210385120, DOI: [10.1073/pnas.2210385120](https://doi.org/10.1073/pnas.2210385120).
- 83 J. Shen, B. Xu, Y. Zheng, X. Zhao, H. Qi, Y. Tang, W. Lin, S. Li and Z. Zhong, Near-Infrared Light-Responsive Immunomodulator Prodrugs Rejuvenating Immune Microenvironment for “Cold” Tumor Photoimmunotherapy, *Angew. Chem., Int. Ed.*, 2025, **64**(22), e202425309, DOI: [10.1002/anie.202425309](https://doi.org/10.1002/anie.202425309).
- 84 Z. Ding, X. Yin, Y. Zheng, Y. Li, H. Ge, J. Feng, Z. Wang, S. Qiao, Q. Sun, F. Yu, Z. Hou, Y.-X. Fu and Z. Liu, Single Atom Engineering for Radiotherapy-Activated Immune Agonist Prodrugs, *Nat. Commun.*, 2025, **16**(1), 6021, DOI: [10.1038/s41467-025-60768-4](https://doi.org/10.1038/s41467-025-60768-4).
- 85 X. Yin, Z. Ding, L. Yu, X. Zhang, Y. Gao, Y. Li, Z. Liu and Y.-X. Fu, Orchestrating Intratumoral DC-T Cell Immunity for Enhanced Tumor Control *via* Radiotherapy-Activated TLR7/8 Prodrugs in Mice, *Nat. Commun.*, 2025, **16**(1), 6020, DOI: [10.1038/s41467-025-60769-3](https://doi.org/10.1038/s41467-025-60769-3).
- 86 H. O. McDevitt, Discovering the Role of the Major Histocompatibility Complex in the Immune Response, *Annu. Rev. Immunol.*, 2000, **18**, 1–17, DOI: [10.1146/annurev.immunol.18.1.1](https://doi.org/10.1146/annurev.immunol.18.1.1).
- 87 R. Al-Daccak, N. Mooney and D. Charron, MHC Class II Signaling in Antigen-Presenting Cells, *Curr. Opin. Immunol.*, 2004, **16**(1), 108–113, DOI: [10.1016/j.coi.2003.11.006](https://doi.org/10.1016/j.coi.2003.11.006).

